J. Physiol. (1982), **329**, *pp.* 263–280
With 1 plate and 10 text-figures
Printed in Great Britain

ENHANCEMENT OF IONIC CURRENTS THROUGH VOLTAGE-GATED CHANNELS IN THE MOUSE OOCYTE AFTER FERTILIZATION

BY NAOHIDE YAMASHITA

From the Laboratory of Neurobiology, Institute of Brain Research, School of Medicine, University of Tokyo, Japan

(*Received 18 November 1981*)

SUMMARY

1. The changes of voltage-gated ion channels in the mouse oocyte after fertilization were investigated under voltage clamp.

2. About 60 min after introduction of sperm suspension into the fertilization medium, the amplitude of inward current through Ca^{2+}-channels increased, which occurred at anaphase during the second meiotic division. The peak amplitude of the maximum inward current per unit membrane capacity of the oocytes at metaphase was $20 \pm 3\ \mu A/\mu F$ in 50 mM-Sr medium. It was $28 \pm 8\ \mu A/\mu F$ at anaphase, and $32 \pm 5\ \mu A/\mu F$ at telophase. The kinetic properties as well as selectivity among Ca, Sr and Mn ions were not altered after fertilization.

3. The outward surge current which was found at the higher membrane potential over +50 mV also increased in amplitude after fertilization, simultaneously with the increase in amplitude of inward current through Ca^{2+}-channels. The means and the standard deviations of the surge current per unit membrane capacity at 120 mV were $31 \pm 8\ \mu A/\mu F$ at metaphase, and $48 \pm 7\ \mu A/\mu F$ at telophase. The kinetic properties of the outward surge current were not altered after fertilization.

4. Application of colcemid (10^{-7} mole/l.) or cytochalasin B (2×10^{-5} mole/l.) did not prevent the increase in amplitude of both inward current through Ca channels and the outward surge current.

5. The membrane currents in N-18 mouse neuroblastoma cells in logarithmic growth phase were examined under voltage clamp. The N-18 neuroblastoma cells possessed the Ca inward current and the delayed outward current. The kinetic properties and the steady-state inactivation of Ca^{2+}-channels in N-18 neuroblastoma cells were compared with those in mouse oocytes. It was concluded that they could be regarded as identical between the mouse oocyte and the N-18 neuroblastoma cell.

INTRODUCTION

The surface membrane of the mouse oocyte undergoes various changes after fertilization, including release of cortical granules (Fukuda & Chang, 1978), changes in concanavalin A binding capacity (Graham, 1974), and reduction of fluidity (Johnson & Edidin, 1978). These changes have also been observed in the sea urchin oocyte (Johnson & Epel, 1975; Mazia, Schatten & Steinhardt, 1975; Steinhardt,

Zucker & Shatten, 1977; Baker & Whitaker, 1978; Epel, 1978; Campisi & Scandella, 1980). In tunicate oocyte, some electrical properties change after fertilization (Kozuka & Takahashi, 1982). On fertilization the oocyte first gains potential, and later the amplitude of the inward current through Na^+-channels increases while that through Ca^{2+}-channels decreases. The increase in amplitude of Na^+-channel current was suggested to be due to appearance of new Na^+-channels on the surface membrane. Apparently, the re-organization of the oocyte membrane after fertilization is accompanied by changes in the number of voltage-gated ion channels.

In a previous paper (Okamoto, Takahashi & Yamashita, 1977), it has been reported that in the unfertilized mouse oocyte, membrane depolarization causes an inward current carried exclusively through Ca^{2+}-channels. No Na current is observed. Upon depolarization beyond +50 mV, there is in addition an outward surge current possibly carried by K ions. Thus, the mouse oocyte possesses at least two voltage-gated ion channels, and shows electrical excitability as found in tunicate and sea urchin oocytes. The present work examines, firstly, what changes occur in the voltage-gated channels immediately after fertilization. Secondly, Ca^{2+}-channels in oocytes are compared quantitatively with those of mouse neuroblastoma cells, and are shown to have almost identical properties (see also Moolenaar & Spector, 1979*b*). This is of interest because the *undifferentiated* neuroblastoma cells studied here may be considered to represent a developmental stage intermediate between the oocyte and the differentiated excitable membranes.

METHODS

Materials and method for fertilization

Eight- to twelve-week-old DDy mice were used. The procedure for superovulation has been described in a previous paper (Okamoto *et al.* 1977). The technique for *in vitro* fertilization of the mouse oocyte was essentially the same as described by Toyoda, Yokoyama & Hoshi (1971*a*). The composition of the medium for *in vitro* fertilization of the mouse oocyte is shown in Table 1. The medium was covered with paraffin oil and had been incubated at 37 °C under 5 % CO_2 in air for a few hours before experiment. A drop of sperm was obtained from cauda epididymides and suspended in 0·4 ml. of the medium. The fresh sperm was incubated in the medium for 2 hr before insemination, because it is known that this procedure (capacitation of spermatozoa) facilitates the spermatozoa to penetrate the oocytes (Toyoda, Yokoyama & Hoshi, 1971*b*). The unfertilized oocytes were collected from the ampulla of the oviduct at 13–16 hr after injection of human chorionic gonadotropine (HCG) and suspended in 0·8 ml. of the medium. The ovulated mouse oocytes have already finished the first meiotic division, releasing the first polar body, and are arrested in metaphase of the second meiotic division. The oocytes do not resume the second meiotic division unless the spermatozoon enters or parthenogenesis occurs. The oocytes in the one side of the oviduct of a mouse were employed for fertilization and the oocytes in the other side of the oviduct were used as a control. Within 10 min after collection of the oocytes, 5–10 μl. of sperm suspension was added to the medium containing oocytes. The final sperm concentration was $50–100 \times 10^3$ cells/ml.

Even though it was ultimately necessary to remove follicular cells around the oocytes before electrical recording, the insemination was carried out with the follicle intact (Toyoda *et al.* 1971*a*), because if the follicular cells were removed with hyaluronidase within 15 min after introduction of sperm suspension, the fertilization rate was found to be considerably reduced and good synchronization for fertilization process among the same batch of oocytes could not be obtained. It has been reported that it takes about 20 min for capacitated spermatozoa to penetrate the zone pellucida in the mouse oocyte (Motomura & Toyoda, 1980). The follicular cells were considered to support the spermatozoa to penetrate the zona pellucida, or the hyaluronidase treatment might

degrade the receptor site for the spermatozoa in zona pellucida (Bledi & Wassarman, 1980). Therefore the follicular cells were removed at over 20 min after introduction of sperm suspension and then the recording from the fertilized oocytes was performed. With this method the fertilization rate was usually over 90% and the synchronization for fertilization was good. The follicular cells of the control oocytes, which were not fertilized, were removed immediately after dissection from the oviduct. The recording for the control oocytes were performed usually within 30 min after

TABLE 1. Ionic composition of media

	Composition of the media for the recording							
	Na (mM)	K (mM)	Ca (mM)	Sr (mM)	Mn (mM)	Mg (mM)	TEA (mM)	Cl (mM)
5 mM-Ca	125·0	6·0	5·0	—	—	1·0	—	138·0
20 mM-Ca	102·5	6·0	20·0	—	—	1·0	—	150·5
20 mM-Sr	102·5	6·0	—	20·0	—	1·0	—	150·5
50 mM-Sr	57·5	6·0	—	50·0	—	1·0	—	165·5
10 mM-Mn	117·5	6·0	—	—	10·0	1·0	—	145·5
25 mM-Mn	95·0	6·0	—	—	25·0	1·0	—	153·0
20 mM-Ca 25 mM-TEA	77·5	6·0	20·0	—	—	1·0	25·0	150·5
50 mM-Sr 25 mM-TEA	32·5	6·0	—	50·0	—	1·0	25·0	165·5

All media were buffered by 20 mM Hepes-Na at pH 7·4 and contained bovine serum albumin (BSA) 10 mg/ml. and glucose 1 mg/ml.

Composition of the medium for the *in vitro* fertilization of the mouse egg: NaCl (119·37 mM), KCl (4·78 mM), $CaCl_2 2H_2O$ (1·71 mM), KH_2PO_4 (1·19 mM), $MgSO_4 7H_2O$ (1·19 mM), $NaHCO_3$ (25·07 mM), Na pyruvate (1·00 mM), glucose (5·56 mM), bovine serum albumin (4 mg/ml.), streptomycin sulphate (0·05 mg/ml.) and penicilline potassium (100 u./ml.).

removal of the follicular cells, because it is known that hyaluronidase treatment may cause parthenogenesis in the mouse oocyte (Graham, 1970; Kaufman, 1973). However, so far as the present experiments were concerned, very few parthenogenetic oocytes were found even more than 3 hr after hyaluronidase treatment, which may be attributed to the relatively early period of collection of oocytes after HCG injection (13–16 hr) and to a medium that kept oocytes in good condition (Graham, 1974). In the present experiment, polyspermic oocytes made less than a few percent, which were all dispermic. The results in dispermic oocytes were not different from those in monospermic oocytes.

Neuroblastoma

Cells of mouse neuroblastoma clone N-18 were cultured in Dulbeco's modified Eagle medium with 10% new born calf serum. The cells were subcultured once in 7–10 days. The culture medium was exchanged two times a week.

Recording

Two glass micro-electrodes (filled with 3 M-KCl) were inserted into cells, one for recording membrane potential, the other for injecting current. For mouse oocytes, electrode resistances were 10–30 MΩ, while for N-18 neuroblastoma cells, they were 30–50 MΩ because the neuroblastoma cells deteriorated rapidly after the insertion of electrodes with low resistance. Relatively large cells (diameter over 20 μm) were selected because these produced larger ionic currents. The techniques for electrical recordings were described in detail by Miyazaki, Ohmori & Sasaki (1975*a*) and Okamoto, Takahashi & Yoshii (1976). When a relatively brief current pulse (5 msec) compared with the time constant of oocyte membrane (about 50 msec) was applied, the membrane potential initially showed an almost linear change, which represented dV/dt. Dividing the value of applied current (I) by that of dV/dt, the membrane capacity was obtained. The holding potential for voltage clamp was −75 mV. The temperature of the bath was kept at 25·5 ± 1 °C. The ionic compositions of the bathing media used for electrical measurement are shown in Table 1. Ca ions

were replaced by Mn ions in the ratio 2:1, since the stabilizing effect of Mn ions was about twice that of these ions.

Histology

Immediately after electrical recording, the micro-electrodes were gently removed from the oocyte. The oocyte was transferred to a glass slide and lightly compressed with cover glass. A mixture of paraffin and vaseline in a ratio of 1:9 containing glass beads of 20 μm diameter were attached on the four corners of the cover glass in advance to avoid crushing the cell. The oocyte was pre-fixed with 5% glutaraldehyde for 5–10 min and then fixed for 24 hr in 10% formaldehyde which was

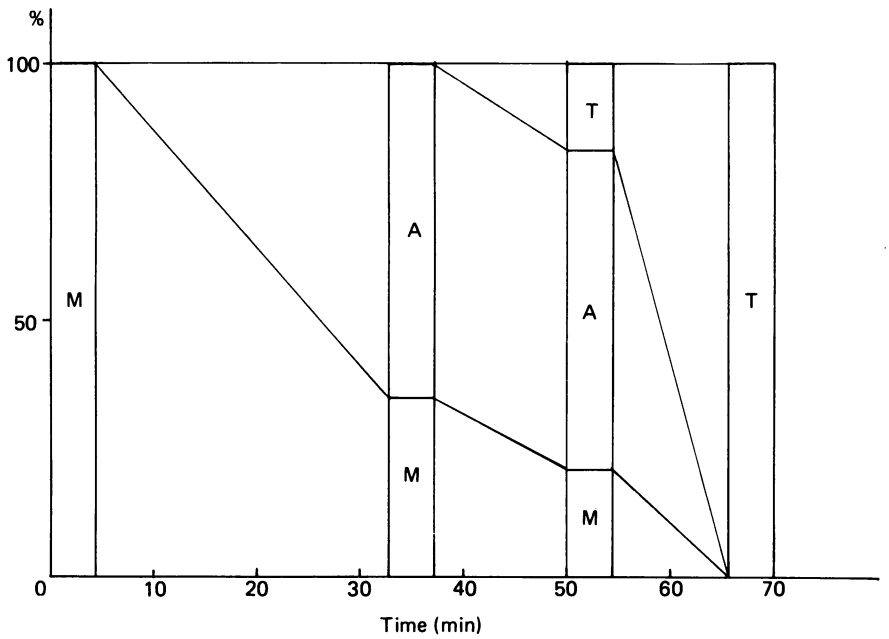

Fig. 1. *In vitro* fertilization of mouse oocytes. Abscissa: time interval from introduction of sperm suspension into the medium to fixation. Ordinate: percentage of oocytes at respective stages during the second meiotic division. M (metaphase) represents the stage at the arrest in the second meiosis. A (anaphase) represents the stage where chromosomes are separating. T (telophase) represents the stage after the mid body is formed. Just after introduction of sperm suspension, all oocytes are at metaphase (n = 13). After 33 min, 37% of the oocytes (11/31) are at metaphase, and 63% of the oocytes (20/31) are at anaphase. After 52 min, 21% at metaphase (6/29), 62% at anaphase (18/29), and 17% at telophase (5/29). At 66 min all oocytes finished the second meiotic division (100% telophase, n = 33).

buffered with 10% KH_2PO_4 at pH 7·4. Then the oocyte was washed in 95% ethanol and stained with 0·25% lacmoid in 45% acetic acid for visualization of the chromosomes and/or the sperm head. It was probable that the development of fertilized oocyte might progress during the recording. However, development should be minimal because the bath temperature was kept at 24·5–26·5 °C and the time interval between the beginning of recording and the prefixation was usually less than 5 min.

In the present experiment, the stage at the arrest in metaphase of second meiosis is represented as metaphase (M). Anaphase (A) represents the stage where the chromosomes were separating toward two poles. Telophase (T) represents the stage after the chromosomes completed the separation and the clearly visible mid body was formed. The photographs of these stages are shown in Pl. 1.

Fig. 1 shows the progress of the second meiotic division of fertilized oocytes after introduction of sperm suspension into the fertilization medium. Immediately after insemination, all oocytes remained at metaphase. After 33 min, the oocytes at the anaphase were 65%. The stage thereafter progressed and after 66 min all oocytes finished the second meiotic division (100% telophase). In the present experiment the fertilized oocytes actually did not divide while the electrical recording was carried out, although the extrusion of the second polar body began at telophase.

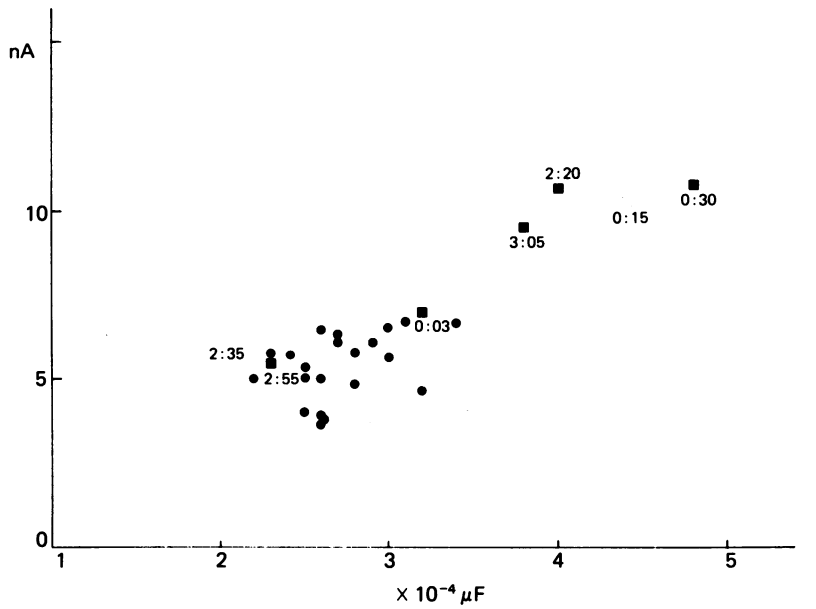

Fig. 2. The relationship between the total membrane capacity and the peak amplitude of the maximum inward current through Ca^{2+}-channels in 50 mM-Sr medium. The records represented by squares are obtained in unfertilized oocytes of a mouse. ■, oocytes which were histologically confirmed as metaphase. □, oocytes which were not histologically examined. Small number at the records indicates the time interval (hours:minutes) from the collection of oocytes to the recording. ●, records of the unfertilized oocytes at metaphase used in the present experiment.

RESULTS

Changes in the voltage-gated channels after fertilization

Membrane capacity and calcium current before fertilization

The total membrane capacity, which represents the surface membrane area, was measured in 121 unfertilized oocytes. The mean and the standard deviation of total membrane capacity was $2{\cdot}48 \pm 0{\cdot}66 \times 10^{-4}$ μF, which was almost identical with the figure ($2{\cdot}5 \pm 0{\cdot}3 \times 10^{-4}$ μF, $n = 5$) obtained in the previous study (Okamoto *et al.* 1977). The mean specific capacitance was estimated as 1·5 μF/cm², assuming the oocyte has a spherical surface with the mean diameter of 72 μm (Okamoto *et al.* 1977). Fig. 2 illustrates the relationship between the total membrane capacity and the peak amplitude of the maximum inward current through voltage-clamped Ca^{2+}-channels in 50 mM-Sr medium. The inward current was measured at −15 mV because it is maximal at that potential.

In the present study, the electrical recording was carried out at temperatures of 25·5 ± 1·0 °C because at the higher temperature over 30 °C the oocytes deteriorated soon after insertion of the electrodes. The amplitude of the inward current through Ca channels at 25 °C became about a half of that at 35 °C. In order to obtain larger currents, inward currents were measured in media containing high concentration

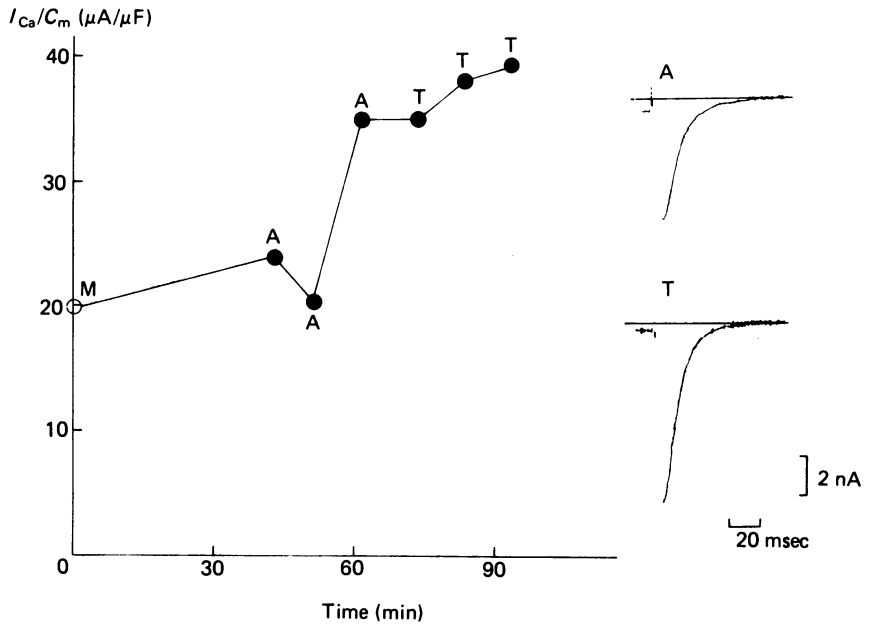

Fig. 3. The change of the peak amplitude of the maximum inward current per unit membrane capacity (I_{Ca}/C_m) during the second meiotic division. M, metaphase; A, anaphase; T, telophase; the record represented by ○ (metaphase) was not histologically examined. However, since it was recorded just after collection from the oviduct, the stage of the oocyte was decided to be metaphase. The insets in the figure represent the records at anaphase (35 min) and at telophase (70 min). All records in 50 mM-Sr medium.

(usually 50 mM) of Sr ions. Another reason for avoiding Ca^{2+} was that repetitive voltage pulses (0·1 Hz) greater than the threshold for Ca^{2+}-channels in 50 mM-Ca medium reduced the amplitude of the inward current without a change in kinetics. This was probably ascribable to an increase in free intracellular Ca^{2+} concentration. However, in 50 mM-Sr medium such a reduction in amplitude of the inward current was very small.

Open and filled squares in Fig. 2 indicate results from unfertilized oocytes obtained from the same mouse. The peak amplitude of maximum inward current was almost linearly related to the total membrane capacity, which implied that the specific current density was almost constant among oocytes from the same mouse. The specific current density was, however, somewhat variable from one mouse to another. Since the present experiment was aimed to examine the changes of ionic currents through voltage-gated ion channels after fertilization, it was necessary to select oocytes which possessed current densities within a certain range. In about 80% of mice, the specific current density per unit membrane area of the unfertilized oocytes

was within a range from 14 to 25 μA/μF, as shown by filled circles in Fig. 2. These mice were employed for the present experiment. The total membrane capacity of these control oocytes was in a range from 1·2 to $3{\cdot}8 \times 10^{-4}$ μF ($\bar{x} \pm 2\sigma$) (the histogram of total membrane capacity formed an almost normal distribution).

The small numbers attached to the squares in Fig. 2 indicate the time interval (hours:minutes) from the dissection of the oviduct to recording. It was found that

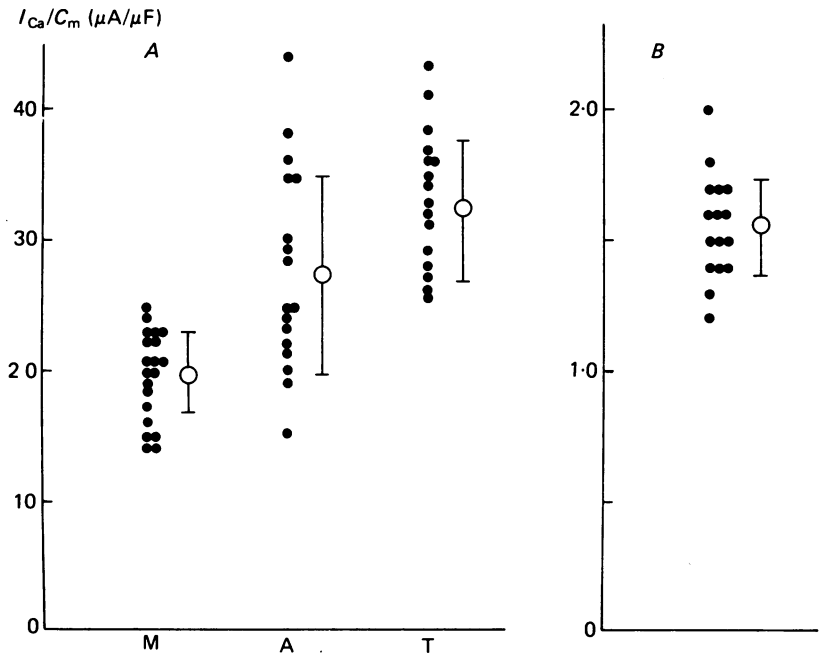

Fig. 4. *A*, summarized plots of the peak amplitude of the maximum inward current per unit membrane capacity (I_{Ca}/C_m). Each ● indicates the record from a single oocyte. ○ and bars represent the means and standard deviations. Recorded in 50 mM-Sr medium. *B*, the ratios of I_{Ca}/C_m at telophase to the mean of I_{Ca}/C_m at metaphase in the same mouse.

the specific current density was not changed during 3 hr after hyaluronidase treatment in unfertilized oocytes remaining at metaphase.

Increase in amplitude of inward currents through Ca^{2+}-channels after fertilization

Fig. 3, left, illustrates the changes of the peak amplitude of the maximum inward current per unit membrane capacity ($I_{Ca^{2+}}/C_m$) through Ca^{2+}-channels after introduction of sperm suspension into the medium. Each point was obtained from an oocyte. The oocyte at 0 min was unfertilized and obtained from one side of the oviduct, the other oocytes were fertilized and obtained from the other side of the oviduct in the same mouse. After introduction of sperm suspension $I_{Ca^{2+}}/C_m$ at first did not significantly change, while the second meiotic division advanced to anaphase, but between 42 and 55 min inward current grew 1·8 fold. Histological examination revealed that this growth occurred in late anaphase. After 55 min the second meiotic division progressed to telophase, and inward current showed no further change. Fig. 3,

right, illustrates records of maximum inward current at anaphase (at 35 min) and at telophase (at 70 min). Kinetically, inward current appeared almost identical in both stages. Other experiments confirmed that the increase in inward current took place mostly during anaphase.

Fig. 4*A* summarizes results from other similar experiments and shows $I_{Ca^{2+}}/C_m$ at metaphase, at anaphase and at telophase. At metaphase the mean and standard

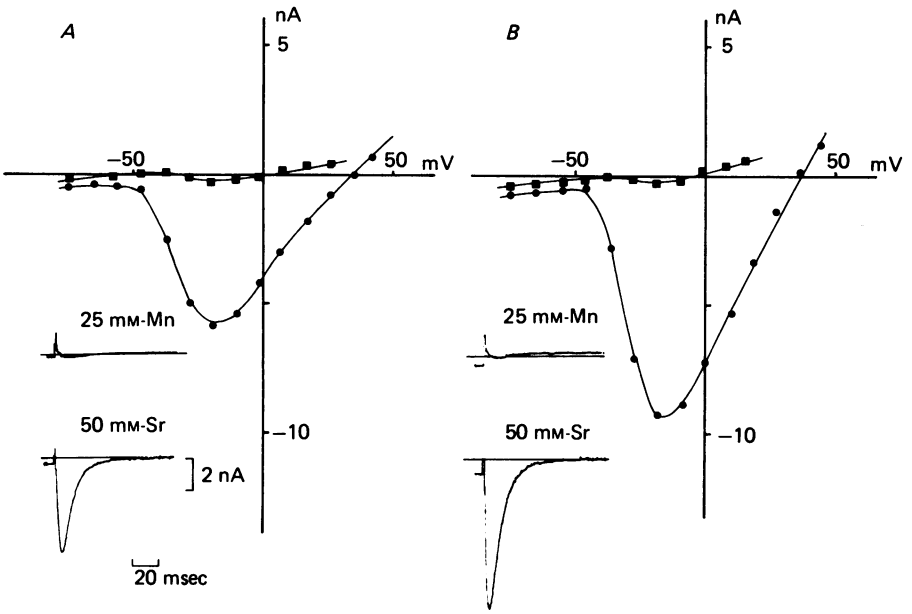

Fig. 5. *V–I* relations for the peak inward currents. *A*, at metaphase; *B*, at telophase. ●, records in 50 mM-Sr medium. ■, in 25 mM-Mn medium. The insets illustrate the records at the maximum peak inward current in respective media.

deviation of $I_{Ca^{2+}}/C_m$ was $20\pm3\ \mu A/\mu F$ ($n = 20$). At anaphase it was $28\pm8\ \mu A/\mu F$ ($n = 17$). At telophase it was $32\pm5\ \mu A/\mu F$ ($n = 16$). The standard deviation at anaphase was greater than those at metaphase and at telophase because the increase in amplitude of the inward current usually occurred during anaphase. $I_{Ca^{2+}}/C_m$ at telophase was about 1·6 times as large as that at metaphase. The difference was statistically significant ($P \ll 0{\cdot}01$). Then, $I_{Ca^{2+}}/C_m$ at telophase was divided by the mean of $I_{Ca^{2+}}/C_m$ at metaphase in the same mouse and was plotted in Fig. 4*B*. The mean increase ratio of inward current through Ca^{2+}-channels was 1·6, which was identical with the value in Fig. 4*A*. The increased ratios of $I_{Ca^{2+}}/C_m$ recorded in other media (20 mM-Ca, 20 mM-Sr, 5 mM-Ca) than 50 mM-Sr, were similarly 1·6–1·8. The distribution of the total membrane capacity of the oocytes did not significantly differ at any stage in the second meiosis. This indicated that the membrane capacity of the mouse oocyte did not change after fertilization, as in case of the tunicate oocyte (Kozuka & Takahashi, 1981).

The *V–I* relations for Ca-channel current in 50 mM-Sr and 25 mM-Mn solutions at metaphase and at telophase are shown in Fig. 5. The potential of the threshold, the peak, and the reversal were almost identical in both stages. The potential levels of

the maximum inward current (V_p) and the potential levels at which the peak inward current attained its half maximum ($V_{\frac{1}{2}}$) were $-14{\cdot}7 \pm 1{\cdot}7$ mV (V_p) and $-32 \pm 1{\cdot}8$ mV ($V_{\frac{1}{2}}$) at metaphase ($n = 22$), and $-13{\cdot}6 \pm 1{\cdot}7$ mV (V_p) and $-31{\cdot}2 \pm 1{\cdot}6$ mV ($V_{\frac{1}{2}}$) at telophase ($n = 13$). Replacement of Sr or Ca solution with Mn solution almost completely abolished the inward current but a very small inward current remained

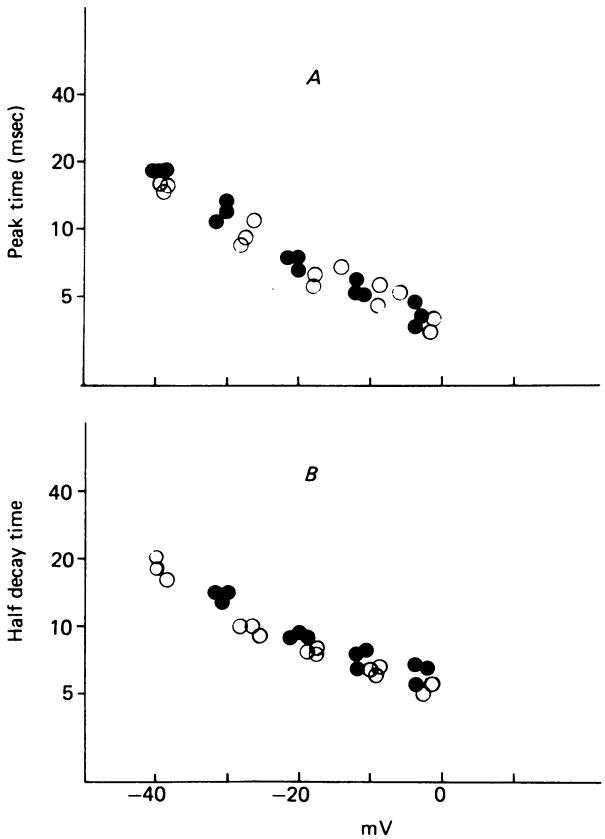

Fig. 6. Dependence of the time course of inward current upon membrane potential. *A*, the peak time (the time from initiation of voltage pulse to the peak of the inward current) against membrane potential. *B*, half decay time (the time from the peak to the half decay) against membrane potential. ●, at metaphase. ○, at telophase.

at both stages. In Fig. 6 the time-to-peak and the half inactivation time of the inward current in 50 mM-Sr solution are plotted against voltage. These values were not significantly different between metaphase and telophase. Therefore it was concluded that in the mouse oocyte the amplitude of the inward current through Ca^{2+}-channels increased after fertilization and that kinetic properties of Ca^{2+}-channels were not altered.

Increase in amplitude of outward surge current after fertilization

In a previous paper (Okamoto *et al.* 1977) it was reported that there was an outward current in the unfertilized mouse oocyte. The inset in Fig. 7*A* illustrates examples

of the outward current at metaphase and at telophase, which were recorded at the potential level of 115 mV. The peak amplitude of the outward current at telophase was about 1·5 times that at metaphase, whereas the steady level was slightly decreased at telophase. The time-to-peak and the half decay time of the surge current (the total outward current minus the steady current) at metaphase were almost the

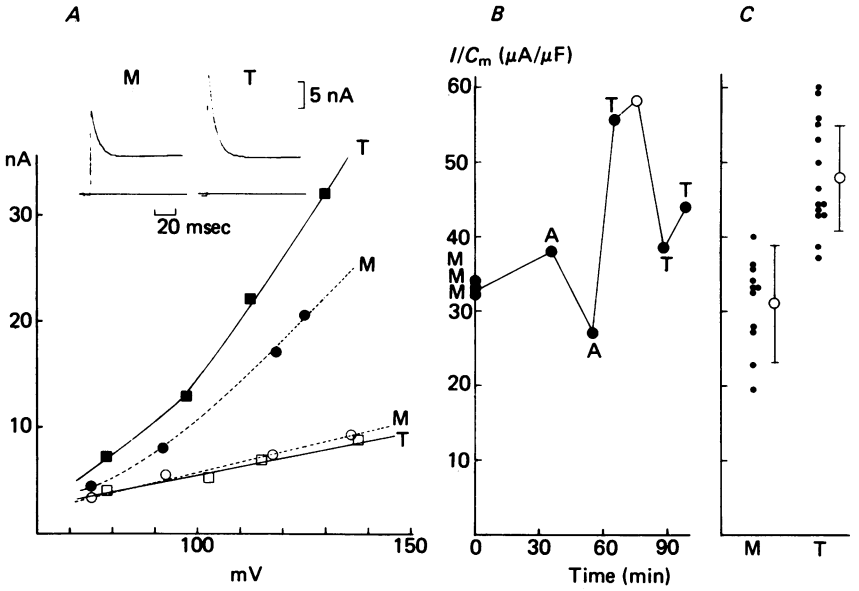

Fig. 7. The change of the outward surge current after fertilization. *A*, *V–I* relation of the outward current of the oocytes at metaphase (dashed line) and at telophase (continuous line). Filled symbols represent the peak amplitude of the outward current. Open symbols, the steady current. The insets illustrate the records of oocytes at metaphase and at telophase at the potential level of 115 mV. *B*, the change of the surge current (the peak amplitude of the outward current minus the steady current) at the potential level of 120 mV per unit membrane capacity (I/C_m) during the progress of second meiotic division. The record at 70 min was not histologically examined. *C*, summarized data of I/C_m of the surge current at 120 mV. Each filled circle from a single oocyte. ○ and bars, the means and the standard deviations. In 50 mM-Sr medium.

same as those at telophase. As in the case of the inward current, the kinetic properties of the surge current appeared not to be changed after fertilization.

Fig. 7*A* plots steady (open symbols) and peak currents (filled symbols) against potential, including values measured before (M) and after fertilization (T). Values at 120 mV were obtained from such plots by interpolation. Fig. 7*B* plots the difference between peak and steady outward current at 120 mV, and shows that this difference increased at 60 min after introduction of sperm suspension into the medium, simultaneously with the increase in amplitude of the inward current through Ca-channels. As before, the unfertilized oocytes at metaphase were obtained from one side of the oviduct and the fertilized oocytes from the other. The amplitude of the surge current at anaphase was not increased in this particular experiment but the increase was usually observed during anaphase. Fig. 7*C* summarizes results obtained in many experiments as in Fig. 7*B*. The mean and the standard deviation of the surge

current per unit membrane capacity (I/C_m) at metaphase was 31 ± 8 μA/μF ($n = 11$) and at telophase it was 48 ± 7 μA/μF ($n = 14$). The mean amplitude of I/C_m at telophase was about 1·5 times that at metaphase. Although the amplitude of the surge current in telophase was relatively scattered, the difference was statistically significant ($P \ll 0{\cdot}01$). The results so far show that both outward and inward current increase in amplitude after fertilization without a change in kinetics.

The effect of colcemid and cytochalasin B on the change of voltage-gated ion channels

Colcemid and cytochalasin B have been known to inhibit various cytokinetic phenomena by interfering with the elements in cytoskeleton, such as microtubules and microfilaments. Application of these agents in a low concentration into the fertilization medium did not reduce the fertilization rate, or precisely speaking, the penetration rate of the spermatozoon into the vitelline membrane. In the presence of colcemid (10^{-7} mole/l.) which interferes with microtubules, the chromosomes of the fertilized oocyte remained at metaphase, while the penetrated sperm head formed a male pronucleus. The oocyte appeared at a glance to be fertilized but failed to resume the second meiotic division. However, the amplitude of the inward current through Ca^{2+}-channels as well as the outward surge current increased at 1 hr after introduction of sperm suspension into the medium. In the presence of cytochalasin B (2×10^{-5} mole/l.) which interferes with microfilaments, the oocyte failed to release the second polar body and three pronuclei were formed in the fertilized oocyte. The inward current as well as the outward surge current increased in amplitude at 1 hr after introduction of sperm suspension into the medium, which was the same as in case of application of colcemid.

Comparison of inward currents in oocytes and the N-18 neuroblastoma cells

Fig. 8 illustrates a series of membrane currents in N-18 neuroblastoma cells recorded in 50 mM-Sr medium under voltage clamp. As in mouse oocytes, recording was carried out in medium containing a high concentration of divalent cations. This increased current amplitudes, and if Sr^{2+} was used, the reduction in amplitude of the inward current after repetitive stimulation (0·1 Hz) was very small. The inward current appeared at about -50 mV, reaching maximal peak amplitude at about -20 mV. During potential steps beyond -20 mV the delayed outward current followed the initial inward current. The amplitude of the outward current increased with the larger depolarization, as did the rates of activation and inactivation. Similar inward and outward currents were observed in 20 mM-Ca medium, with thresholds being almost the same as in 50 mM-Sr medium. The inward current was nearly abolished by replacement of Sr or Ca solution with Mn solution, though a very small inward current remained (inset in Fig. 8*B*). On the basis of the time course, the small residual inward current in 25 mM-Mn medium probably flowed through Ca^{2+}- rather than Na^+-channels (see Moolenaar & Spector (1978) for time course of Na^+-currents). Residual small currents possibly carried by Mn ions were also observed in the mouse oocyte (see above). The *V–I* relation at the peak of the inward current in the N-18 neuroblastoma cell is shown as filled circles in Fig. 8*B*. Open circles indicate the *V–I* relation of the inward current in the unfertilized mouse oocyte (see Fig. 5*A* for comparison). Both the potential level of the maximum peak inward current and the

apparent reversal level for the initial current were more negative than in the mouse oocyte. However, the difference may be due to the delayed outward current in the N-18 neuroblastoma cell. If outward current was suppressed by 25 mM-external TEA, the *V–I* relation in the N-18 neuroblastoma cell became almost the same as that in the mouse oocyte. Therefore it was concluded that the *V–I* relations for the inward

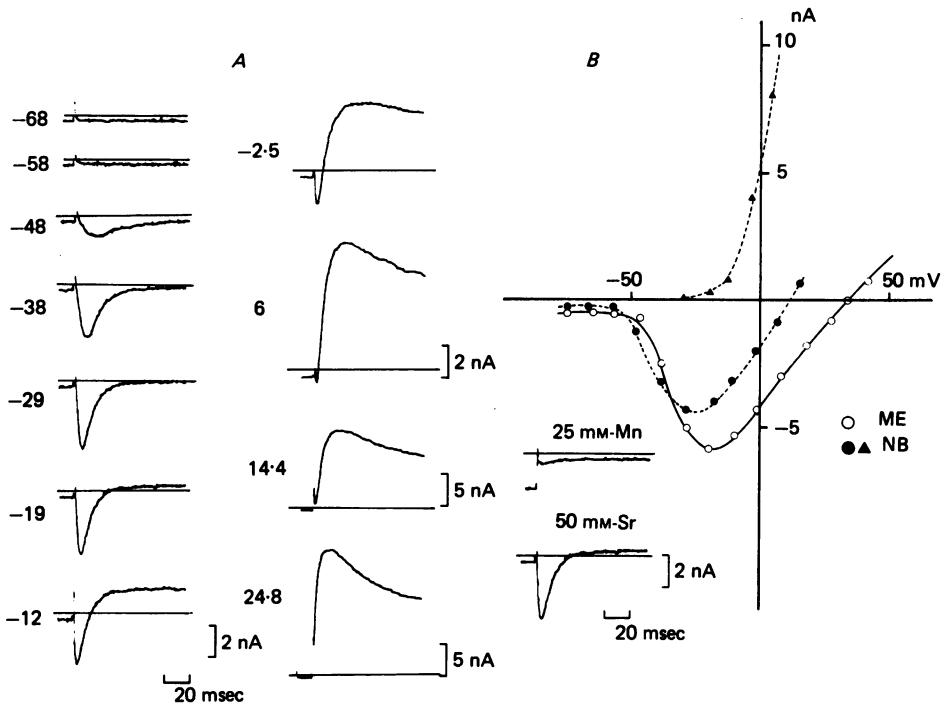

Fig. 8. Membrane currents and their *V–I* relations in the N-18 mouse neuroblastoma cell. *A*, membrane currents in 50 mM-Sr medium under voltage clamp. The amplitude of membrane currents in this cell was the largest in the present experiment. *B*, *V–I* relations at the peak of the inward current (● and dashed line) and at the peak of the outward current (▲ and dashed line). ○ and the continuous line indicate the *V–I* relation of an unfertilized mouse oocyte. The insets illustrate the inward currents of the N-18 neuroblastoma cell in 50 mM-Sr medium and in 25 mM-Mn medium. Potential at −19 mV.

current through Ca^{2+}-channels were essentially identical between the oocyte and the N-18 neuroblastoma cell, as previously described in case of the artificially differentiated neuroblastoma cell by Moolenaar & Spector (1979*b*). Unlike in the artificially differentiated neuroblastoma cells (Miyake, 1978; Kostyuk, Krishtal, Pidoplichko & Vaselovsky, 1978; Moolenaar & Spector, 1978), there appeared to be no component of Na-current in the N-18 neuroblastoma cells.

Steady state inactivation curves and kinetic properties of the Ca^{2+}-channels

For precise comparison of Ca^{2+}-channels in oocytes and in N-18 neuroblastoma cells, further analysis was necessary. The time courses of the inward current through Ca^{2+}-channels do not differ among Ca^{2+}, Sr^{2+} and Ba^{2+} ions in the mouse oocytes,

and the *V–I* curve in Mn media does not show rectifications between −250 and +50 mV (Okamoto *et al.* 1977). In N-18 neuroblastoma cells, the time courses of the inward current did not differ between Ca^{2+} and Sr^{2+} ions (see also Moolenaar & Spector (1979*b*) for records in Ca^{2+}, Sr^{2+} and Ba^{2+} ions), and the remarkable rectifications were not found below +20 mV when the delayed outward current was

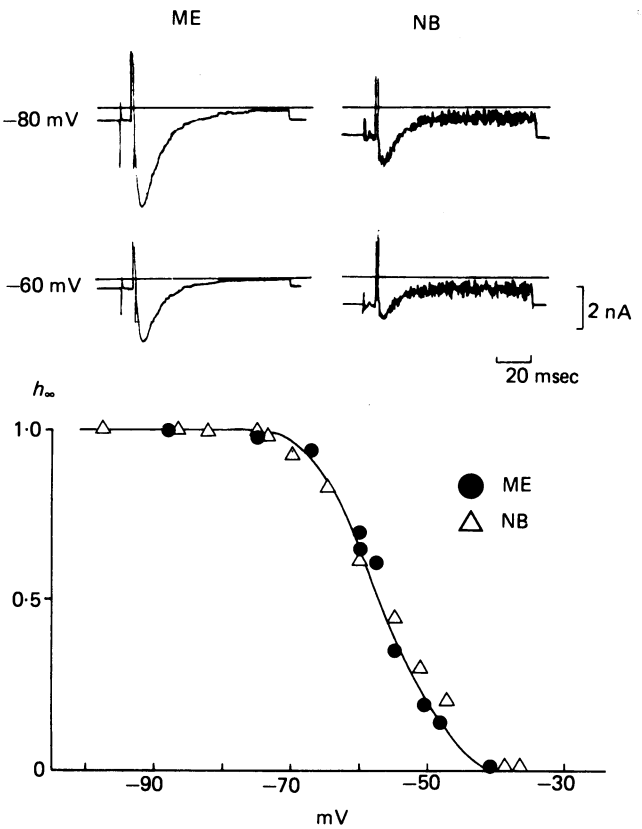

Fig. 9. Steady-state inactivation curve of the inward current through Ca^{2+}-channels. Abscissa: holding potential. Ordinate: the ratio of the peak inward current at the test potential level of −15 mV to the largest value with the hyperpolarized holding level of −90 mV. ●, from the oocyte at metaphase (ME). △, from the N-18 neuroblastoma cell (NB). The insets illustrate example records in the oocyte and in the N-18 neuroblastoma cell at the holding potentials at −80 and −60 mV. The test potential was −15 mV.

suppressed by external TEA. In the present experiment, therefore, the contribution of Ca^{2+}-induced Ca^{2+}-channel inactivation (Brehm & Eckert, 1978; Tillotson, 1979; Ashcroft & Stanfield, 1981) as well as outward currents including Ca^{2+}-induced K^+-current (Meech, 1978) were considered to be negligible in the following analysis.

The properties of steady-state inactivation process of inward current through Ca^{2+}-channels were examined by stepping from various holding potential to a fixed level of −15 mV. The inward currents were corrected for leakage current and the inactivation was measured by normalizing the largest peak amplitude of i_{Ca} at

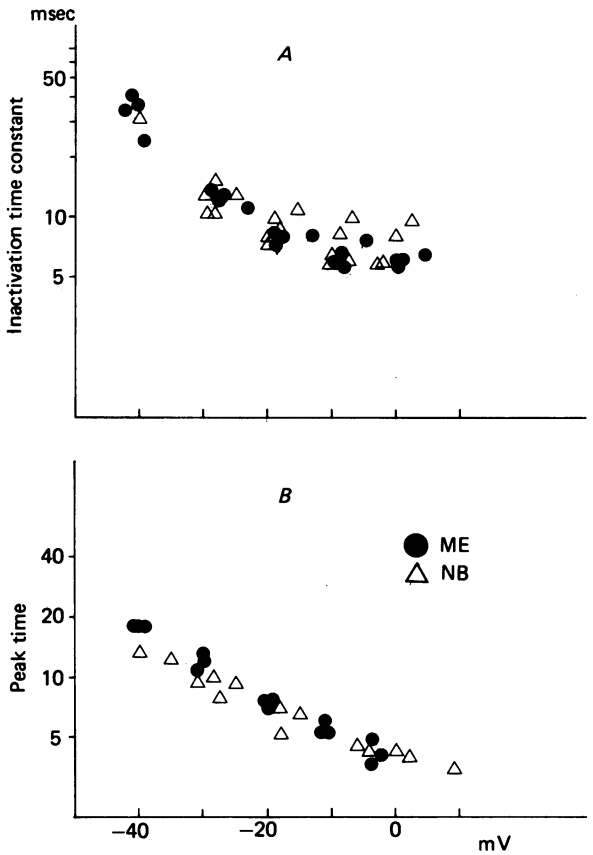

Fig. 10. Potential dependence of kinetic parameters of Ca^{2+}-channels. *A*, inactivation time constant (τ_h) of the inward current against membrane potential. *B*, the peak time of the inward current against membrane potential. In 50 mM-Sr medium. Temp. 26·5 °C. ●, the mouse oocyte at metaphase. △, and N-18 neuroblastoma cell.

−15 mV to one. Fig. 9 shows the example records of the inward current at −80 mV and at −60 mV, and the steady-state inactivation curve. The solid line was drawn according to the formula

$$h_\infty = 1\Big/\left(1+\exp\frac{V-V_{h-\frac{1}{2}}}{K_h}\right),$$

where V is the holding potential and $V_{h-\frac{1}{2}}$ is the potential level at which h_∞ becomes 0·5 (−57 mV). The slope parameter K_h is set to 4·8 mV, which is the same as reported in case of Ca^{2+}-channel in artificially differentiated neuroblastoma cell (Moolenaar & Spector, 1979*b*). The steady state inactivations in the oocyte and in N-18 neuroblastoma cell were almost identical.

The inactivation time course of the inward current, after the correction for leakage current at different potential steps, was examined by plotting the inward current in a semilogarithmic scale. The decaying phase fitted the straight line, indicating the

kinetics followed a first-order process with a single time constant (τ_h), which is plotted against the membrane potential in Fig. 10*A*. The data in N-18 neuroblastoma cell were rather scattered, but it could be regarded that τ_hs of Ca^{2+}-channels in oocytes and in N-18 neuroblastoma cells were almost the same. For the activation process, the time to peak of the inward current is plotted in Fig. 10*B*. It was almost the same between the mouse oocyte and N-18 neuroblastoma cell. Therefore it was concluded that kinetic properties of Ca^{2+}-channels in oocytes and in N-18 neuroblastoma cells were almost identical.

DISCUSSION

The present results revealed that in the mouse oocyte the amplitude of the ionic currents through voltage-gated channels increased about 50–60 min after insemination. Histological examination confirmed that these changes occurred at anaphase during the second meiotic division, which indicated that the amplitude of the ionic currents increased slightly later than the attachment of the spermatozoon on the vitelline membrane. The time required for the capacitated spermatozoa to penetrate zona pellucida has been reported to be about 20 min in the mouse oocyte (Motomura & Toyoda, 1980). Therefore the change in ionic currents took place about 30–40 min after attachment of the spermatozoon on the vitelline membrane.

Possible mechanism of increase in amplitude of the ionic currents through voltage-gated channels after fertilization

In tunicate it has been suggested that the increase in amplitude of Na-current after fertilization was due to appearance of new Na-channels on the surface membrane (Kozuka & Takahashi, 1981). In the case of Ca^{2+}-channels in the mouse oocyte, the specific current density increased after fertilization and kinetic properties as well as *V–I* relations of voltage-gated channels did not alter, suggesting that the increase of ionic currents is also ascribable to an increase in the number of channels. Since the increase occurs about 30–40 min after fertilization, *de novo* synthesis of channel protein might be responsible. Another explanation may be that the increase in amplitude of the ionic currents is due to the appearance of already existing channels on the cell membrane. The application of drugs that interfere with the elements of cytoskeleton, such as colcemid or cytochalasin B, did not prevent the increase in amplitude of ionic currents after fertilization. However, analogous results with Con A binding sites (Graham, 1974), micro-exocytosis of channels, or unmasking of cryptic channels seem possible, if these mechanisms are resistant to colcemid or cytochalasin B.

Similarity of Ca channels in the mouse oocyte and the undifferentiated neuroblastoma cell

Moolenaar & Spector (1978, 1979*a*, *b*) have analysed Na, Ca, and K-channels in N_1 E-115 mouse neuroblastoma cells differentiated by DMSO. They have reported that the Ca channels in the artificially differentiated neuroblastoma cells are very similar to those in the unfertilized mouse oocyte, with respect to selectivity among alkaline earth cations, the threshold, peak and reversal potentials in the *V–I* curve, and the time course of the inward current. The present results extend this similarity to

undifferentiated neuroblastoma cells. This suggests that during differentiation from oocyte to nerve cells, the properties of Ca^{2+}-channels remain essentially unchanged. The density of current through Ca^{2+}-channels in both mouse oocytes and N-18 neuroblastoma cells was calculated to be from 3×10^{-5} to 2×10^{-4} A/cm^2 in 50 mM-Sr medium, which may be comparable with the value of Ca^{2+}-channels in the artificially differentiated neuroblastoma cells in 20 mM-Ca medium, considering that the amplitude of inward currents in 50 mM-Sr medium was about 1·7 times of that in 20 mM-Ca medium (Moolenaar & Spector, 1979*b*).

The threshold and the kinetics of the outward current in the N-18 neuroblastoma cell were similar to those in the artificially differentiated neuroblastoma cell (Moolenaar & Spector, 1979*b*). TEA seems to have a similar pharmacological effect upon differentiated and undifferentiated cells. However, the maximum conductance ($\bar{G}_K$) per unit membrane area in the present work was less than 10% of that reported in the artificially differentiated neuroblastoma cells. The Na^+-current was never found in the membrane of the N-18 neuroblastoma cell under voltage clamp, in contrast to the high density of Na^+-current in the artificially differentiated neuroblastoma cell (Moolenaar & Spector, 1978). The threshold and the kinetics of the delayed outward current in the N-18 neuroblastoma cell was different from that in the oocyte, in contrast to the constancy of the inward current through Ca^{2+}-channels. During development, K^+-channels may thus change more than Ca^{2+}-channels.

Functional significance of Ca^{2+}-channels

The resting potential of unfertilized oocytes recorded with a single electrode of a high resistance over 60 MΩ is about −40 mV in standard medium, and after fertilization the resting potential becomes about 20 mV more negative (S. Miyazaki & Y. Igusa, personal communication). In the present experiments the steady-state inactivation curve of Ca^{2+}-channels overlapped the descending limb of the *V–I* curve between −50 and −35 mV in 50 mM-Sr medium, as had been suggested by Moolenaar & Spector (1979*b*). Since $V_{\frac{1}{2}}$ in 50 mM-Sr medium was 15 mV more positive than in standard medium (Okamoto *et al.* 1977), the region of overlap is probably from −65 to −50 mV in standard medium, and encompasses the resting potential of the fertilized oocyte. Therefore, it is possible that some proportion of Ca^{2+}-channels will be steadily open in fertilized oocytes, and that inward flux of Ca ions will be enhanced by the addition of Ca^{2+}-channels. The role of Ca ions at fertilization has been considered in many studies, and includes the release of cortical granules (Baker & Whitaker, 1978; Steinhardt *et al.* 1977), and the decrease of the membrane fluidity after fertilization (Campisi & Scandella, 1980). Ca^{2+} influx of sufficient magnitude can even cause parthenogenesis (Fulton & Whittingham, 1978). Thus it is possible that the inward flux of Ca ions through Ca^{2+}-channels can take part in the re-organization of the unfertilized oocyte into a dividing cell.

In the cultured dorsal root ganglion cells, it has been reported that the maximum rate of rise of Ca spike increases during neurite outgrowth (Fukuda & Kameyama, 1979). During maturation of the starfish oocyte it has been also reported that the maximum rate of rise of Ca action potential increases following breakdown of germinal vesicles (Miyazaki, Ohmori & Sasaki, 1975*b*), when the first meiotic division starts. Although these experiments are carried out by current clamp technique, the

increase of maximum rate of rise of Ca^{2+} action potential can be interpreted by an increase in number of Ca^{2+}-channels. All above reports together suggest that the number of Ca^{2+}-channels often increases before the surface membrane expands in the course of growth, be it in preparation for polar body formation during meiosis or during neurite outgrowth.

I would like to thank Professor K. Takahashi for his aid and advice throughout this research and in preparing the manuscript, and Professor H. Shimazu for reading the manuscript and offering valuable criticism. I also thank Professor Y. Toyoda for teaching the method for *in vitro* fertilization of mouse oocytes. N-18 cloned mouse neuroblastoma cell was the thankful gift from Dr K. Ikeda.

REFERENCES

ASHCROFT, F. M. & STANFIELD, P. R. (1981). Calcium dependence of the inactivation of calcium currents in skeletal muscle fibres of an insect. *Science, N.Y.* **213**, 224–226.

BAKER, P. F. & WHITAKER, M. J. (1978). Influence of ATP and calcium on the cortical reaction in sea urchin eggs. *Nature, Lond.* **276**, 513–515.

BLEIL, J. D. & WASSARMAN, P. M. (1980). Mammalian sperm-egg interaction: identification of a glycoprotein in mouse egg zona pellucidae possessing receptor activity for sperm. *Cell* **20**, 873–882.

BREHM, P. & ECKERT, B. (1978). Calcium entry leads to inactivation of calcium channel in *Paramecium*. *Science, N.Y.* **202**, 1203–1206.

CAMPISI, J. & SCANDELLA, C. J. (1980). Calcium-induced decrease in membrane fluidity of sea urchin egg cortex after fertilization. *Nature, Lond.* **286**, 185–186.

EPEL, D. (1978). Mechanisms of activation of sperm and egg during fertilization of sea urchin gametes. *Curr. Top. dev. Biol.* **12**, 185–249.

FUKUDA, K. & CHANG, M. C. (1978). The time of cortical granule breakdown and sperm penetration in mouse and hamster eggs inseminated in vitro. *Biol. Reprod.* **19**, 216–266.

FUKUDA, J. & KAMEYAMA, M. (1979). Enhancement of Ca spikes in nerve cells of adult mammals during neurite growth in tissue culture. *Nature, Lond.* **279**, 546–548.

FULTON, B. P. & WHITTINGHAM, D. G. (1978). Activation of mammalian oocytes by intracellular injection of calcium. *Nature, Lond.* **273**, 149–151.

GRAHAM, C. F. (1970). Parthenogenetic mouse blastocysts. *Nature, Lond.* **226**, 165–167.

GRAHAM, C. F. (1974). The production of parthenogenetic mammalian embryos and their use in biological research. *Biol. Rev.* **49**, 399–422.

JOHNSON, M. & EDIDIN, M. (1978). Lateral diffusion in plasma membrane of mouse egg is restricted after fertilization. *Nature, Lond.* **272**, 448–450.

JOHNSON, J. D. & EPEL, D. (1975). Relationship between release of surface proteins and metabolic activation of sea urchin eggs at fertilization. *Proc. natn. Acad. Sci. U.S.A.* **72**, 4474–4478.

KAUFMAN, M. H. (1973). Parthenogenesis in the mouse. *Nature, Lond.* **242**, 475–476.

KOSTYUK, P. G., KRISHTAL, O. A., PIDOPLICHKO, V. I. & VESELOVSKY, N. S. (1978). Ionic currents in the neuroblastoma cell membrane. *Neuroscience* **3**, 327–332.

KOZUKA, M. & TAKAHASHI, K. (1982). Changes in holding and ion-channel currents during activation of an ascidian egg under voltage clamp. *J. Physiol.* **323**, 267–286.

MAZIA, D., SCHATTEN, G. & STEINHARDT, R. (1975). Turning on of activities in unfertilized sea urchin eggs: correlation with changes of the surface. *Proc. natn. Acad. Sci. U.S.A.* **72**, 4469–4473.

MEECH, R. W. (1978). Calcium-dependent potassium activation in nervous tissue. *A. Rev. Biophys. Bioeng.* **7**, 1–18.

MIYAKE, M. (1978). The development of action potential mechanism in a mouse neuronal cell line in vitro. *Brain Res.* **143**, 349–354.

MIYAZAKI, S., OHMORI, H. & SASAKI, S. (1975*a*). Action potential and non-linear current-voltage relation in starfish oocytes. *J. Physiol.* **246**, 37–54.

MIYAZAKI, S., OHMORI, H. & SASAKI, S. (1975*b*). Potassium rectifications of the starfish oocyte membrane and their changes during oocyte maturation. *J. Physiol.* **246**, 55–78.

MIYAZAKI, S. & IGUSA, Y. (1981). Fertilization potential in golden hamster eggs consists of recurring hyperpolarization. *Nature, Lond.* **290**, 702–704.

MOOLENAAR, W. H. & SPECTOR, I. (1978). Ionic currents in cultured mouse neuroblastoma cells under voltage-clamp conditions. *J. Physiol.* **278**, 265–286.

MOOLENAAR, W. H. & SPECTOR, I. (1979*a*). The calcium action potential and a prolonged calcium dependent after-hyperpolarization in mouse neuroblastoma cells. *J. Physiol.* **292**, 297–306.

MOOLENAAR, W. H. & SPECTOR, I. (1979*b*). The calcium current and the activation of a slow potassium conductance in voltage-clamped mouse neuroblastoma cells. *J. Physiol.* **292**, 307–323.

MOTOMURA, M. & TOYODA, Y. (1980). Scanning electron microscopic observations on the sperm penetration through the zona pellucida of mouse oocyte fertilized in vitro. *Jap. J. Zootech. Sci.* **51**, 595–601.

OKAMOTO, H., TAKAHASHI, K. & YOSHII, M. (1976). Membrane currents of the tunicate egg under the voltage-clamp condition. *J. Physiol.* **254**, 607–638.

OKAMOTO, H., TAKAHASHI, K. & YAMASHITA, N. (1977). Ionic currents through the membrane of the mammalian oocyte and their comparison with those in the tunicate and sea urchin. *J. Physiol.* **267**, 465–495.

STEINHARDT, R., ZUCKER, R. & SCHATTEN, G. (1977). Intracellular calcium release at fertilization in the sea urchin egg. *Devl Biol.* **58**, 185–196.

TILLOTSON, D. (1979). Inactivation of conductance dependent on early entry of Ca ions in molluscan neurons. *Proc. natn. Acad. Sci. U.S.A.* **76**, 1497–1500.

TOYODA, Y., YOKOYAMA, M. & HOSHI, T. (1971*a*). Studies on the fertilization of mouse eggs *in vitro*. I. *In vitro* fertilization of eggs by fresh epididymal sperm. *Jap. J. Anim. Reprod.* **16**, 147–151.

TOYODA, Y., YOKOYAMA, M. & HOSHI, T. (1971*b*). Studies on the fertilization of mouse eggs *in vitro*. II. Effects of *in vitro* preincubation of spermatozoa on time of sperm penetration of mouse eggs *in vitro*. *Jap. J. Anim. Reprod.* **16**, 152–157.

EXPLANATION OF PLATE

Mouse oocytes during the second meiotic division, photographed under a phase-contrast microscope. Pre-fixed with 5% glutaraldehyde, fixed with 10% formaline, stained with 0·25% lacmoid in 45% acetic acid. Magnification × 320. *A*, an unfertilized oocyte at metaphase. The chromosomes remain at metaphase II (arrow). *B*, a fertilized oocyte examined at about 30 min after introduction of sperm suspension. The chromosomes are arranged at the equator line (arrow). The oocyte up to this stage is included in metaphase in the present experiment. *C*, a fertilized oocyte showing the chromosomes at anaphase II (arrow). About 40 min after introduction of sperm suspension. *D*, a fertilized oocyte at telophase II (arrow), fixed at about 60 min after introduction of sperm suspension. *E*, the penetrated spermatozoon (lower) forms an enlarged head in contrast to the unpenetrated spermatozoon (upper). Examined at about 70 min after insemination. *F*, male and female pronuclei (arrows). The nucleus of the second polar body is out of focus. Fixed at about 5 hr after insemination.

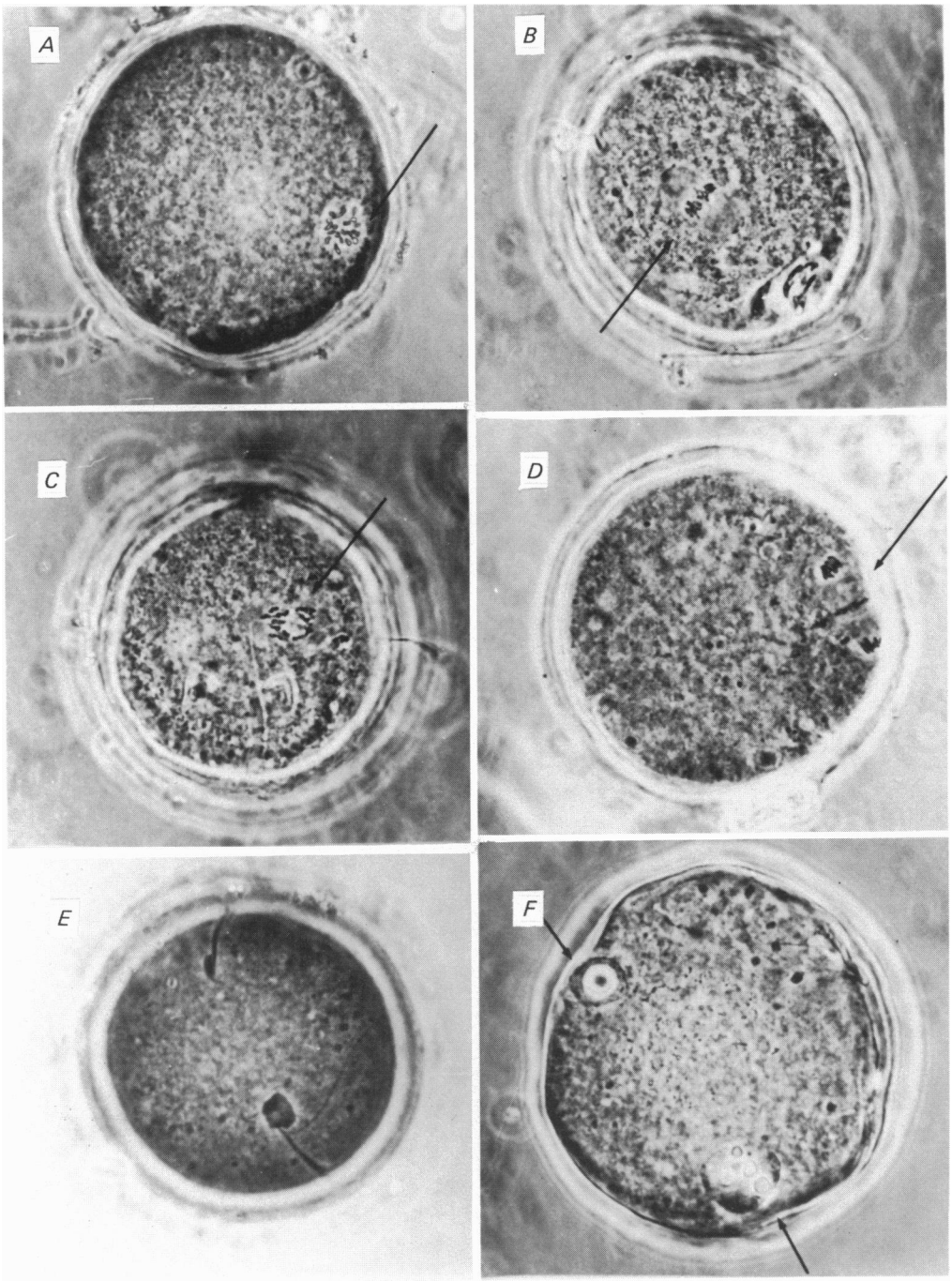
A
B
C
D
E
F